Much of Zero Emissions Commitment Occurs Before Reaching Net Zero Emissions

Charles D. Koven[1*], Benjamin M. Sanderson[2], Abigail L. S. Swann[3]

1. Climate and Ecosystem Sciences Division, Lawrence Berkeley National Laboratory, Berkeley, California, USA
2. Centre for International Climate and Environmental Research (CICERO), Oslo, Norway
3. Department of Atmospheric Science and Department of Biology, University of Washington, Seattle, WA, USA

***Email:** cdkoven@lbl.gov

Abstract

We explore the response of the Earth's coupled climate and carbon system to an idealized sequential addition and removal of CO_2 to the atmosphere, following a symmetric and continuous emissions pathway, in contrast to the discontinuous emissions pathways that have largely informed our understanding of the climate response to net zero and net negative emissions to date. We find, using both an Earth System Model and an ensemble of simple climate model realizations, that warming during the emissions reduction and negative emissions phases is defined by a combination of a proportionality of warming to cumulative emissions characterized by the Transient Climate Response to Emissions (TCRE), and a deviation from that proportionality that is governed by the Zero Emissions Commitment (ZEC). About half of the ZEC is realized before reaching zero emissions, and the ZEC thus also controls the timing between peak cumulative CO_2 emissions and peak temperature, such that peak temperature may occur before peak cumulative emissions if ZEC is negative, underscoring the importance of ZEC in climate policies aimed to limit peak warming. Thus we argue that ZEC is better defined as the committed warming relative to the expected TCRE proportionality, rather than as the additional committed warming that will occur after reaching net zero CO_2 emissions. Once established, the combined TCRE and ZEC relationship holds almost to complete removal of prior cumulative CO_2 emissions. As cumulative CO_2 emissions approach zero through negative CO_2 emissions, CO_2 concentrations drop below preindustrial values, while residual long-term climate change continues, governed by multicentennial dynamical processes.

Introduction

Current climate policy is informed by the idea that the magnitude of global warming is proportional to cumulative CO_2 emissions (IPCC 2013, 2021). This relationship emerges from complex interactions between the physics and biogeochemistry of the Earth system, and has been consistently found under scenarios of positive CO_2 emissions (Allen *et al* 2009, Matthews *et al* 2009). The simplicity and path-independence of the relationship allow the creation of a remaining carbon budget consistent with limiting warming to a specific level. However, the path-independence of the relationship between warming and cumulative CO_2 emissions, known as the Transient Climate Response to cumulative CO_2 Emissions (TCRE), is only approximate – for example it is possible that some CO_2-driven temperature change will occur after emissions cease, which can be quantified as the Zero Emissions Commitment (ZEC) (Matthews and Caldeira 2008, Solomon *et al* 2009, Jones *et al* 2019), that is used alongside the TCRE in constructing a remaining carbon budget for climate stabilization for policy applications (Rogelj *et al* 2019).

The modeled proportionality of warming to cumulative emissions, despite emerging from complex and at least partially coincidental interactions (Raupach 2013, Goodwin *et al* 2015, MacDougall and Friedlingstein 2015), holds to a remarkably high amount of cumulative emissions (Tokarska *et al* 2016, Koven *et al* 2022). Likewise, under negative CO_2 emissions, the proportionality of warming to cumulative CO_2 emissions still holds as cumulative emissions decrease, subject to an asymmetry governed by the ZEC (Koven *et al* 2022) in both idealized (Tokarska *et al* 2019) and scenario-driven (Koven *et al* 2022) experiments for overshoots up to ~300 PgC. Thus, a hypothetical framework for highly mitigated scenarios is that long-term warming equals the cumulative emissions times TCRE plus a committed ZEC value, which may hold from net zero to net negative emissions. While the expected time lag between CO_2 emissions and CO_2-driven warming is only about a decade (Ricke and Caldeira 2014), the controls of that lag remain insufficiently quantified. The idealized experiments used to quantify TCRE and ZEC, where TCRE is the warming during the exponential CO_2 concentration growth phase (Arora *et al* 2020) and ZEC is the subsequent warming after emissions instantaneously go to zero (MacDougall *et al* 2020, Jones *et al* 2019) do not allow assessment of when ZEC may occur as emissions decrease on the path to net zero or net negative CO_2 emissions.

It is also not clear how far the relationship between warming, cumulative emissions and ZEC described above would hold under negative emissions. Here we ask whether temperature remains proportional to cumulative emissions, plus a ZEC value, as far as to the removal of all anthropogenic CO_2 emissions in pursuit of restoring the climate system to a preindustrial-like state, which we term a restoration scenario. Previous work on the reversibility of climate change under declining CO_2 has used time-reversed CO_2 concentration scenarios, with either idealized (Boucher *et al* 2012, Zickfeld *et al* 2016, Ziehn *et al* 2020, Keller *et al* 2018, MacDougall 2019) or scenario-driven (John *et al* 2015, MacDougall 2013) experiments. These experiments find asymmetries in the climate and carbon cycle with respect to changing CO_2 concentrations, e.g., that there is a substantial lag between global temperature change and CO_2 concentrations after concentrations reversal (Lee *et al* 2021). While, in general, concentration-

driven experiments can be used to infer emissions and thus frame climate outcomes in terms of compatible emissions, the abrupt reversal from increasing to declining CO_2 concentrations in some of these scenarios requires a highly discontinuous emissions timeseries. For example in the Coupled Model Intercomparison Project phase 6 (CMIP6) Carbon Dioxide Removal Model Intercomparison Project (CDRMIP) 1%/yr concentration reversal, this requires instantly changing emissions by ~50 PgC/yr from large positive to large negative values (fig. S1a). Because the inertia of the Earth system acts like a low-pass filter, it is possible that this abrupt and very large change in emissions, which also holds for pulse CO_2 emission or removal experiments (Ricke and Caldeira 2014, Zickfeld *et al* 2021), pushes the path-independence of the TCRE to the point where it may no longer hold on shorter timescales. For example, in idealized 1%/yr reversal experiments, the proportionality of warming to cumulative emissions does not generally hold, as global temperatures are warmer for a given level of emission during the negative emissions period than during the positive emissions period (Zickfeld *et al* 2016), which we also find for the CMIP6 CDRMIP ensemble mean (fig. S1b). In scenario-based overshoot projections, the transition from positive to negative emissions takes decades (fig. S2), thus such large abrupt emissions changes are unlikely to occur. MacDougall (2019) also argue against the abrupt emissions changes required for exponential concentrations reversals and propose as a solution a logistic CO_2 concentration pathway. We argue that forcing with CO_2 emissions rather than concentrations has a further benefit of more cleanly separating the peak emissions amount and the timing of net zero as independent rather than dependent variables of the scenario design.

We thus design an idealized emissions-driven carbon dioxide removal (CDR) experiment with the following three goals: we seek first to avoid sharp discontinuities in emissions, so as not to break the path-independence of the TCRE relationship or the timing of ZEC emergence due to any such discontinuities; second to have roughly exponential ramp-up of emissions early in the scenario to match the shape of historical emissions, and third to keep emissions symmetric in time before and after net zero to explore asymmetries in carbon fluxes and climate responses with respect to emissions. A simple experimental design that satisfies these criteria is for cumulative CO_2 emissions to follow a Gaussian curve over a given interval, and thus annual emissions follow the first derivative of a Gaussian. We force climate models under this scenario, with cumulative emissions reaching a maximum of 1000 PgC after 150 years of simulation and returning to zero after 300 years (figs 1a-b). This climate restoration experiment allows us to ask three related questions: (1) how would the Earth system respond to the removal of all previously-emitted CO_2 and thus cumulative net zero CO_2 emissions, (2) what are the lags and asymmetries of the transient response of climate and carbon cycle dynamics to a symmetric shift from positive to negative CO_2 emissions, and (3) how does the ZEC impact the relative timing between peak cumulative emissions and peak warming?

Methods

The annual emissions timeseries $E(t)$ [PgC/yr] for year t follows the form of the first derivative of a Gaussian curve:

$$E(t) = \frac{a\,(b-t)\,e^{\frac{-(b-t)^2}{2c^2}}}{c^2}$$

We use values of *a (*maximum cumulative emissions) of 1004 PgC, *b* (year of peak cumulative emissions) of year 150, and *c* (timescale for emissions reversal) of 45. We use *a* of 1004 PgC, rather than 1000 PgC, because the cumulative emissions at year 1 is 4 PgC, thus the total integrated emissions over the period years 1-150 is 1000 PgC, and years 151-300 is -1000 PgC. After year 300, we set annual emissions to zero. Emission fluxes are distributed equally over the planet. Since the magnitude of ZEC is a function of maximum cumulative emissions (MacDougall *et al* 2020), we use the same maximum cumulative emissions (1000 PgC) as the standard Zero Emissions Commitment Model Intercomparison Project (ZECMIP) experiment. This peak cumulative emissions is also close to the value used to calculate TCRE (at 2x CO_2, i.e., year 70 of the 1%/yr idealized concentration run), which minimizes any inconsistencies that might be introduced by calculating these metrics at different amounts of cumulative CO_2 emissions.

We use the CESM2 (Danabasoglu *et al* 2020), version 2.1.3, in an emissions-driven mode, (compset 'B1850_BPRP') with the default initial conditions for the emissions-driven configuration (year 151 of (CESM developers 2019)). For the transient simulation, all non-CO_2 aspects of the model were kept at constant preindustrial values, and CO_2 concentrations were prognostic in response to the specified emissions timeseries. Output fluxes and climate variables were smoothed using an 11-year Savitzky-Golay filter to remove interannual variability.

We conduct a large Perturbed Parameter Ensemble (PPE) using the FaIR 1.3 simple climate model (Smith *et al* 2018, Millar *et al* 2017). We use 1000 ensemble members, with model radiative forcing parameters sampled following (Smith *et al* 2018), with an extended sampling of model thermal and carbon timescale parameters sampled as detailed in Tables S1-S3, where parameter ranges are informed by a number of studies exploring the emulation of Earth System Models with an impulse response formulation (Proistosescu and Huybers 2017, Rugenstein and Armour 2021, Caldeira and Myhrvold 2013). Ensemble configurations are filtered according to their ability to reproduce historical global temperature pathways as in (Thompson *et al* 2015), leaving 207 filtered ensemble members. For each ensemble member, we calculate the response to the idealized CDR pathways, as well as standard emissions-driven metrics of TCRE (MacDougall 2016) and ZEC (MacDougall *et al* 2020). TCRE is here calculated as the warming in year 70 of a concentration driven simulation (where concentrations increase from pre-industrial levels at 1 percent per year until concentrations are doubled in approximately year 70) divided by compatible emissions (E_{1pct}) derived using an inverse FaIR simulation (Smith *et al* 2018). ZEC is calculated by running the forward model with (E_{1pct}) until year 70, with zero emissions thereafter (Jones *et al* 2019). ZEC_{50} and ZEC_{100} are measured as the temperature change between year 70 and years 120 and 170 respectively.

Results

Carbon fluxes between the atmosphere and both the land and ocean in the CESM2 simulations follow emissions, with both land and ocean sinks changing sign to become sources after the reversal from positive to negative CO_2 emissions (figure 1a). Lags, as quantified by the interval of maximum lagged correlation, between emissions and sinks are longer for the land (20 years) than the ocean (11 years), with the combined land and ocean sink in between (16 years). At the time of maximum cumulative emissions, the lag in land and ocean sinks with respect to emissions means that the sinks are still positive, and thus the atmospheric CO_2 concentration is already declining before emissions reach zero. Thus peak concentrations occur before zero emissions, and more generally, this means that the rate of change of atmospheric CO_2 leads emissions, here by 13 years. This result—that atmospheric CO_2 change leads emissions by approximately the same timescale that sinks lag emissions—follows from the general trigonometric identity for the phase of summed functions if both emissions and sinks follow sinusoidal curves (SI text). The lead of atmospheric growth rate relative to emissions is consistent with that between diagnosed fossil fuel emissions in SSP scenarios that reach net zero as reported by (Liddicoat *et al* 2020) where, e.g. in the SSP5-3.4-overshoot scenario, CO_2 concentrations peak in 2062, while net fossil CO_2 emissions reach zero between 2068-2078, depending on the model.

Integrated CO_2 fluxes (figure 1b) show asymmetries in carbon pools between the positive and negative emissions periods. In particular, at the point of reaching zero cumulative emissions near the end of the experiment, the cumulative atmospheric sink is negative, i.e. CO_2 concentrations are below the preindustrial value, reaching a minimum value of 258 ppm, versus an initial value of 289 ppm and maximum value of 506 ppm (fig. 2a). Land carbon at the end is also slightly below the preindustrial value, with the excess carbon in the ocean. Looking further at the partitioning of carbon within the land and ocean systems (figs.1c-d) shows the excess carbon is at depth, with shallow ocean DIC anomalies following closely the atmospheric timeseries and lag increasing with depth. Thus, even though the ocean shows a shorter lag than the land with respect to flux correlations against emissions, the difference at the end of the simulations is greater. The positive emissions pulse is able to propagate more fully into the deep ocean than the negative emissions pulse, leading to the positive ocean carbon difference at the end of the simulation. On land, there is a difference in lags between vegetation and soil carbon (fig 1d), as well as an asymmetric response in that both lose carbon after peak emissions more rapidly than they gained carbon prior to the peak, following the asymmetry of atmospheric CO_2 concentrations. At the end of the simulation, most carbon lost from land relative to the start of the scenario comes from vegetation rather than soil carbon pools (fig 1d). Zonal-mean land carbon changes (fig. S3) show a stronger latitudinal dependence to the timing of soil carbon than vegetation carbon responses, and some net loss of soil carbon from high latitudes.

The phasing between the physical climate and CO_2 emissions (fig. 2a) shows that global mean surface temperature leads the CO_2 emissions, with a maximum correlation at lead of 5 years. This happens because atmospheric CO_2 concentrations lead emissions by more than the physical climate lags CO_2 concentrations. This result is consistent with, though stronger than,

the current policy framework that reaching zero emissions will lead to effectively immediate stabilization of CO_2-driven global warming. Here, the suggestion from CESM2 is that CO_2-driven temperature stabilization may actually occur before reaching net zero CO_2 emissions. Global precipitation anomalies lag both temperature and CO_2 emissions (fig. 2a). CESM2 has a particularly strongly negative ZEC_{50} value of -0.31°C, which may be manifesting fairly soon after the emissions peak and decline, as was also found in the comparison between ZEC diagnosed from instantaneous transition to net zero versus gaussian emissions (MacDougall *et al* 2020).

As described above, the hypothesis here is that long-term warming after achieving net negative emissions equals the sum of cumulative emissions (CE) times TCRE, plus a committed ZEC value (Koven *et al* 2022). Thus we expect that CESM2, which has a strongly negative ZEC_{50} value of -0.31°C (MacDougall *et al* 2020), will have an equally negative overshoot asymmetry, i.e. with colder temperatures for a given amount of cumulative emissions after reaching net negative emission than before. This is roughly what we find (figure 2b). For most of the positive emissions period, temperature follows the expected proportionality given the previously-reported value of TCRE for the model of 2.13 °C/EgC (Arora *et al* 2020), however, the model falls off the $\Delta T = TCRE * CE$ line after emission rates begin to decline from their maximum values, and relaxes towards a line representing $\Delta T = TCRE * CE + ZEC$, and then follows that line from the point of reaching net negative emissions through almost all the way until net cumulative CO_2 emissions are back to zero. After that point, global mean surface temperatures begin to rise again, even though cumulative emissions continue to fall to zero.

The increase in temperatures at the end of the CESM2 simulation, as cumulative emissions approach zero, shows a distinct regional pattern, with maximum cooling in mid-high northern latitudes at years 200-250, followed by a reversal to warming afterwards (fig. S4a). The spatial pattern and timing relative to the reversal of CO_2 emissions is consistent with that of CESM2 for the SPP5-3.4-overshoot scenario, due to a re-strengthening of AMOC after its transient weakening with warming, where it is the only CMIP6 model to show such behavior (Koven *et al* 2022). A similar dynamic occurs here, but even more so, with AMOC strengthening above its preindustrial value in response to the negative emissions (fig. S4b). Thus the long-timescale warming reflects interactions between the direct forced temperature changes from CO_2 with the indirect response of AMOC and associated heat transport.

Any single Earth system model represents only one estimate of the complex dynamics of the Earth system. To understand more generally how the carbon-climate sensitivity metrics TCRE and ZEC govern the transient dynamics of the Earth system to emissions reversal, we perform a PPE of the Finite Amplitude Impulse Response (FaIR) simple climate model (Smith *et al* 2018) using the same emissions. We find that the 10-90th percentile range of global mean surface temperature variation in response to the forcing broadly follows the pattern of the CESM2 simulation (fig 3a). Differences between CESM2 and the FaIR ensemble are strongest at the end of the experiment, when CESM2 shows a pronounced warming due to AMOC restrengthening (a process not included in FaIR), while the FaIR simulations show a range of

responses, from cooling to warming. Figure 3(b-g) shows scatterplots of TCRE and ZEC for each ensemble against key climate response variables. Peak warming is highly correlated with TCRE (fig. 3b-c), the lag between peak emissions and peak warming is governed primarily by ZEC (fig. 3d-e), and a weak control by ZEC on the temperature change at the end of the simulation (fig. 3f-g). We find that using both TCRE and ZEC in a multivariate linear prediction of end of simulation warming provides no additional predictive skill over using ZEC alone (not shown).

We show when different combinations of sensitivity metrics (i.e. TCRE and ZEC at different timescales) have the strongest predictive power by plotting temperature versus cumulative emissions for each of the FaIR PPE simulations and noting when the minimum spread across the ensemble occurs (fig. 4), which is equivalent to asking when each normalization explains the most variance in temperature across the ensemble Normalizing the warming of each FaIR ensemble member by that ensemble's TCRE (fig. 4a) shows a minimum ensemble spread (vertical dashed lines) midway through the positive emissions phase, with spread increasing as cumulative emissions approach their maximum. Normalizing warming by TCRE plus half of the ZEC_{50} for each ensemble member (fig. 4b) moves the minimum ensemble spread to the point of maximum cumulative emissions, i.e. half of the ZEC has already manifested in these simulations at the point of reaching zero emissions (fig. S5). Normalizing by TCRE plus either ZEC_{50} (fig. 4c) or ZEC_{100} (fig. 4d) shifts the point of minimum ensemble spread to either early (fig. 4c) or midway (fig. 4d) in the negative emissions period, showing that the timescale by which ZEC is quantified governs when in the negative emissions phase that sensitivity is realized.

The experiment here is only one realization from a wide set of possible idealized CO_2 emissions reversibility experiments. Key variables that may affect the carbon and climate response are the total peak emissions and the timescale for emissions growth and reversal. We use FaIR to explore how the dynamics may vary in response to these alternate emissions trajectories (fig. 5). We find: (1) that the transient drop in CO_2 concentrations below preindustrial values near the end of the simulation is robust with respect to variation in the timescale and amplitude within the range explored here (fig. 5b, 5e); (2) that the peak warming amount is roughly insensitive to the timescale of emissions (fig. 5c); (3) that there tends to be a minimum in warming late in the period of net negative CO_2 emissions, which is followed by a re-emergence of warming after the negative-emissions phase (fig. 5c, 5f); (4) that the lag between peak emissions and peak warming increases with higher peak cumulative emissions (Zickfeld and Herrington 2015) (fig 5f); and (5) that the long-term warming after emissions reversal is higher with higher peak cumulative emissions (fig. 5f).

Discussion

The Paris agreement calls for stabilization of the global climate at levels well below two degrees Celsius, and IPCC AR6 assesses that such climate stabilization requires reaching net zero CO_2 emissions (IPCC, 2021). Overshoot scenarios are predicated on the idea that we may exceed target warming levels and require net negative CO_2 emissions to cool and then stabilize the

climate system at the agreed warming levels. Significant climate impacts are already evident at the current warming of 1.1 °C. Thus future generations, if they are able to develop the means to generate the large net negative CO_2 emissions required for overshoot, may wish to try to restore the climate system to a preindustrial-like state, rather than stabilize it at some level of warming well above the preindustrial. While it is not clear whether long-term CDR technologies could ever be deployed at the scale necessary to reach net-negative CO_2 emissions (Anderson and Peters 2016), particularly at the scale considered here (Smith *et al* 2015, Fuss *et al* 2018), or, even if they could, whether the deleterious effects of these technologies would outweigh their potential benefits (Fuss *et al* 2018, Hanssen *et al* 2022), it is nonetheless important to understand how the coupled carbon-climate system would respond to a transient reversal from net positive, through net zero, and to net negative CO_2 emissions.

We find that under this restoration scenario the land and ocean carbon sinks follow the trajectories of CO_2 emissions, becoming sources soon after emissions become negative, consistent with overshoot scenarios (Jones *et al* 2016, Koven *et al* 2022). The relative timing of this transition differs between land and ocean: the ocean responds in CESM2 more rapidly than land in its sink-to-source transition, though the ocean also shows a greater stock of carbon at the end of the simulation, and thus a longer memory to carbon perturbations, than the land. This is consistent with pulse experiments, which show that both land and ocean exchange carbon with the atmosphere at multiple timescales (Joos *et al* 2013, Eby *et al* 2009, Archer *et al* 2009), for land due to the sequence of live and dead pools that carbon passes through, and for the ocean due to the strong gradient with depth in timescales of carbon response to atmospheric perturbations, which give the ocean greater continued uptake at long timescales than land.

In this scenario, for both CESM2 and FaIR, the relationship between global mean temperature and emissions can roughly be broken into three phases. In the first phase, temperature change is proportional to cumulative emissions, with a proportionality described by the TCRE ($\Delta T = TCRE * CE$). In the second phase, the influence of the ZEC begins, as the relationship shifts towards one characterized by $\Delta T = TCRE * CE + ZEC$. The second phase begins roughly at the time of peak emissions rates, i.e. well before reaching net zero, and lasts through most of the period of net negative CO_2 emissions and almost towards the point where cumulative emissions reach zero. Because much of the ZEC influence occurs before reaching net zero, its magnitude governs both the timing between peak cumulative emissions and peak temperature as well as the peak warming that is reached. The third phase is characterized by long-term climate and carbon responses that govern the committed temperature change even after all anthropogenic carbon is removed from the system.

ZEC governs several aspects of the global temperature dynamics in this scenario. First, we find a strong relationship between the ZEC and the lag between peak cumulative emissions and peak temperature, such that if ZEC is negative then peak temperature may actually lead peak cumulative emissions. IPCC AR6 assessed that the best estimate of ZEC is 0 ± 0.3 °C, with low confidence in sign (Lee *et al* 2021). If Earth's ZEC is negative, then CO_2-driven climate change

may begin to reverse slightly before reaching net zero CO_2 emissions, sooner than the decade-lag that is currently estimated (Ricke and Caldeira 2014, Lee *et al* 2021), with important implications for policy. Second, ZEC, alongside TCRE, affects the magnitude of peak warming. Third, ZEC governs the asymmetry in the temperature to cumulative emissions relationship between the positive and negative emissions phases, and fourth the long-term warming.

ZEC has typically been described as the committed temperature change expected to occur a given period after reaching net zero CO_2 emissions (MacDougall *et al* 2020, Jones *et al* 2019). If the relationship between temperature and cumulative CO_2 emissions were strictly path-independent, it would follow that ZEC would have to be exactly zero. Thus a nonzero ZEC implies path dependence of the temperature to cumulative emissions relationship, and more generally, ZEC can be thought of as a measure of that path dependence under strong mitigation. The widely-used approximation for the temperature to cumulative emissions relationship is a linear TCRE that is quantified using a 1%/yr increasing concentration experiment (Arora *et al* 2020). Because this is the same experiment that the standard ZEC quantification is made relative to (MacDougall *et al* 2020, Jones *et al* 2019), that ZEC quantification is also consistent with a second definition of ZEC as the committed temperature change relative to expectations from TCRE proportionality at the point of reaching zero CO_2 emissions. This experiment, as well as the Gaussian emissions experiment described in (MacDougall *et al* 2020), show that the second interpretation is more correct, because the ZEC can become evident before reaching net zero when the transition occurs gradually. Put another way, ZEC can't describe the amount of temperature change that is still to occur after reaching net zero when half, or even all in the case of CESM2, of that temperature change actually occurs before reaching net zero emissions. While such a definition of ZEC also subsumes deviations from linearity in the temperature to cumulative emissions relationship as well as path dependencies, within the range of emissions relevant to climate mitigation, the nonlinear contribution, as measured in increasing CO_2 experiments, is expected to be small (Tokarska *et al* 2016) and thus we expect that ZEC should be dominated by path dependencies, which are themselves controlled by interactions between timescales of forcing and response in both physical and carbon cycle feedbacks. In less idealized scenarios, the relative timing between peak warming and peak cumulative CO_2 emissions will also be governed by non-CO_2 greenhouse gasses, in particular the relative emission declines of cooling versus warming short-lived climate pollutants.

There is a consistent relationship between committed global warming and cumulative emissions, which is that committed warming is equal to TCRE times cumulative emissions, plus ZEC. This relationship holds across a wide range of high-mitigation scenarios whether, after reaching peak cumulative CO_2 emissions, subsequent emission rates remain at net zero or become net negative. If net negative CO_2 emissions are both possible and pursued, we should expect temperatures to follow the same TCRE slope in response to those emissions down almost to the point of cumulative net zero CO_2 emissions, underscoring the potential efficacy of net negative CO_2 emissions for restoration of the climate system. Lastly, the result that much of the ZEC may occur by the time of reaching net zero emissions underscores the importance of ZEC, even on the short timescales required to reach net zero in order to reach Paris Agreement

targets, and that better quantifying ZEC is crucial to understand both peak CO_2-driven warming and the relative timing between peak warming and peak cumulative CO_2 emissions.

Figures

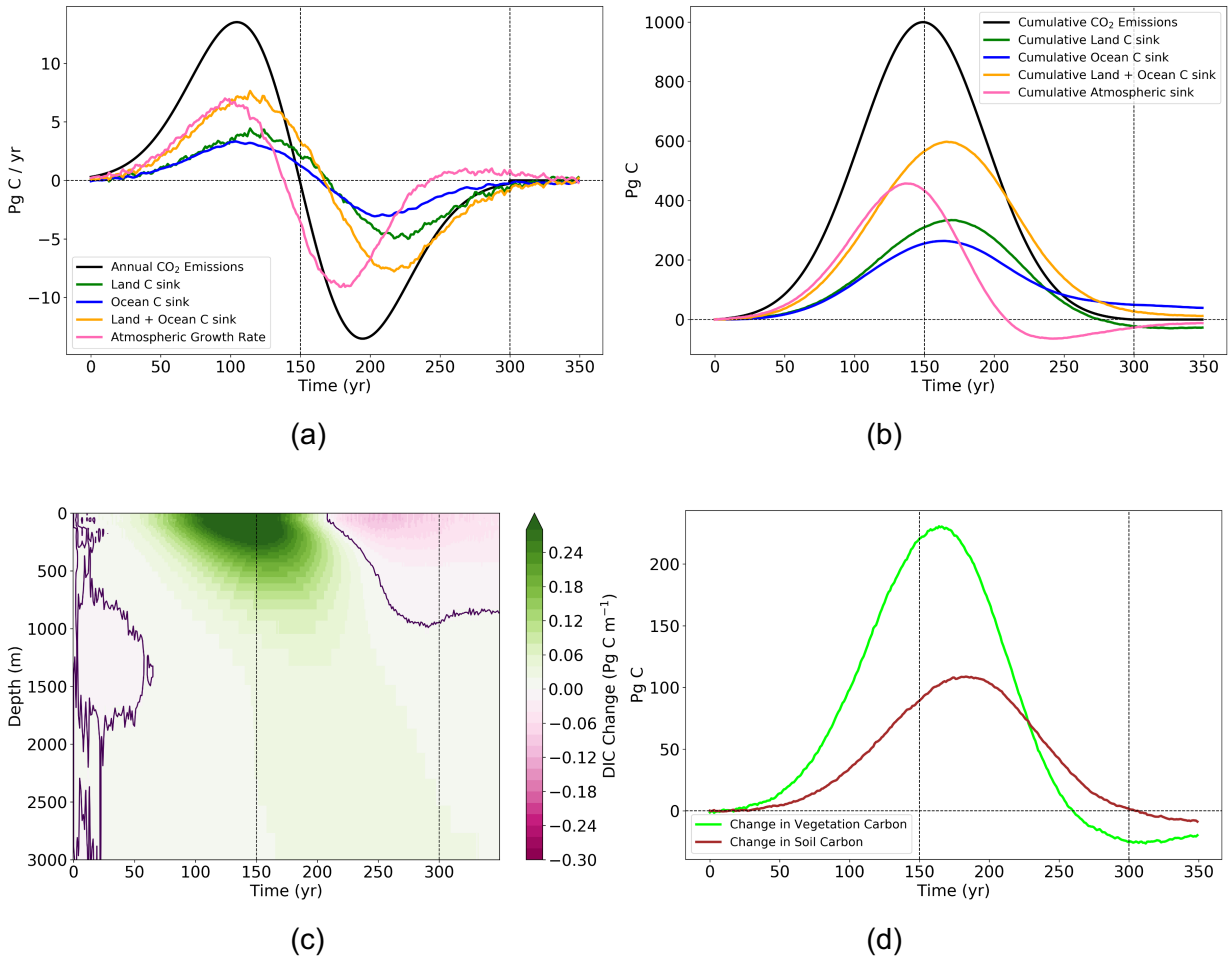

Fig. 1 (a) CO_2 fluxes and (b) integrated CO_2 fluxes in response to the idealized emissions reversal scenario for CESM2. (c) Globally-integrated dissolved inorganic carbon (DIC) stock changes as a function of depth (PgC/m) in the ocean, and (d) Globally-integrated changes in vegetation and soil (including litter and coarse woody debris) carbon stocks (PgC) on land. Vertical dashed lines note times of peak cumulative emissions and return to zero cumulative emissions.

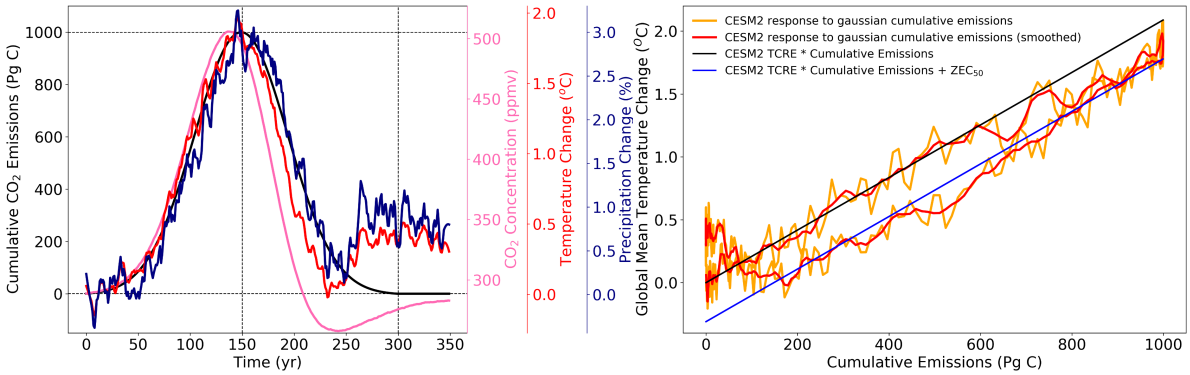

Fig. 2 (a) Timeseries of relative values of CO_2 emissions, global mean CO_2 concentrations, global mean surface temperature anomaly, and global mean precipitation anomaly under the idealized emissions reversal scenario for CESM2. (b) Global warming as a function of cumulative emissions for the scenario. The slope of the black line is the previously-reported value of transient climate response to cumulative CO_2 emissions (TCRE) for CESM2, and the blue line is offset from the black line by the previously-reported value of the 50-year zero emissions commitment (ZEC_{50}) for CESM2. Vertical dashed lines in (a) note times of peak cumulative emissions and return to zero cumulative emissions.

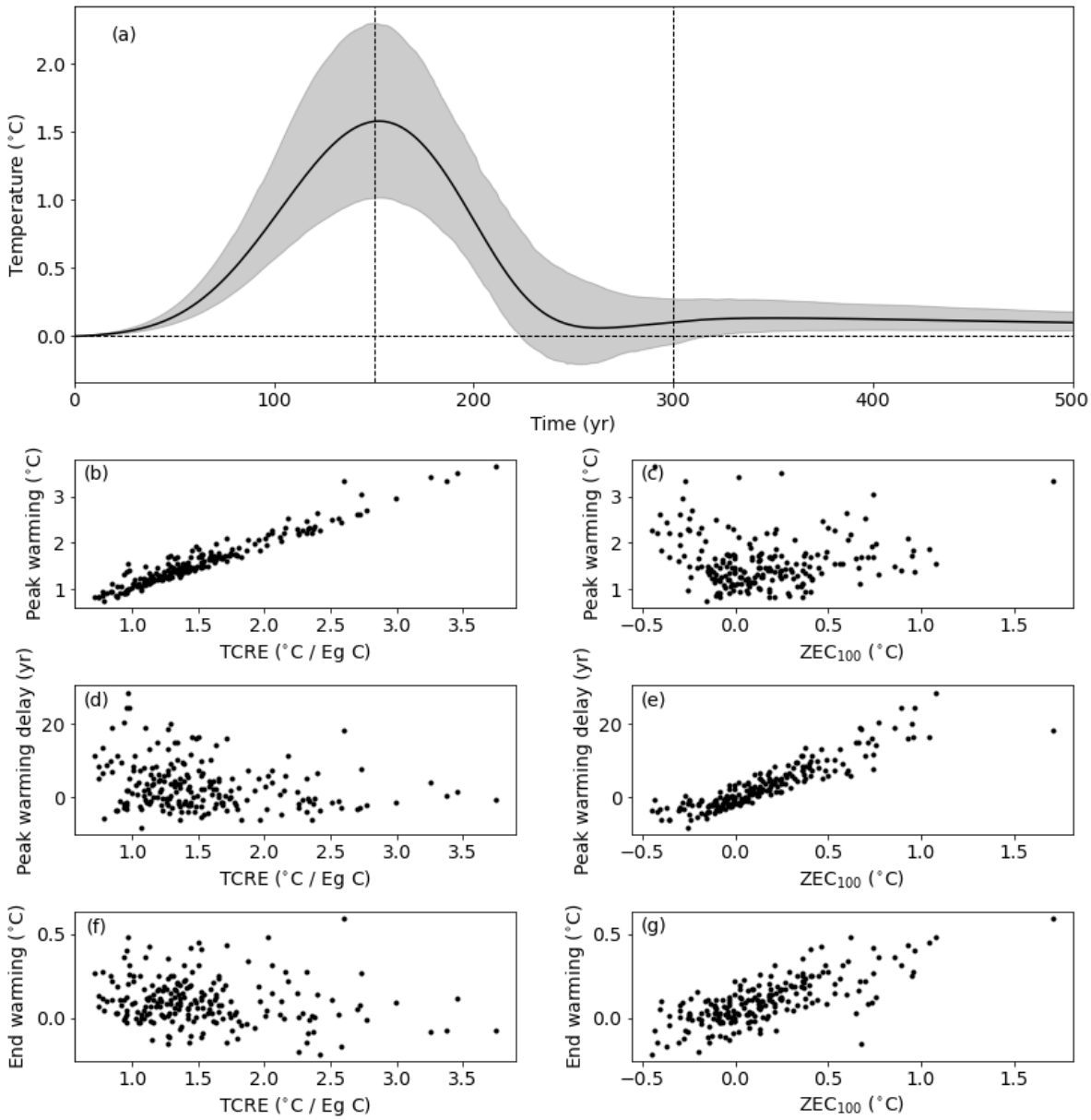

Fig. 3 (a) Range of temperature responses to idealized emissions reversal using an ensemble of FaIR simple climate model realizations. (b-g) Relationship between peak warming, lag of peak temperature to peak warming, and warming at the end of the experiment to the climate sensitivity metrics TCRE and 100-year ZEC (ZEC_{100}), using FaIR simple climate model. Vertical dashed lines in (a) note times of peak cumulative CO_2 emissions and return to zero cumulative emissions.

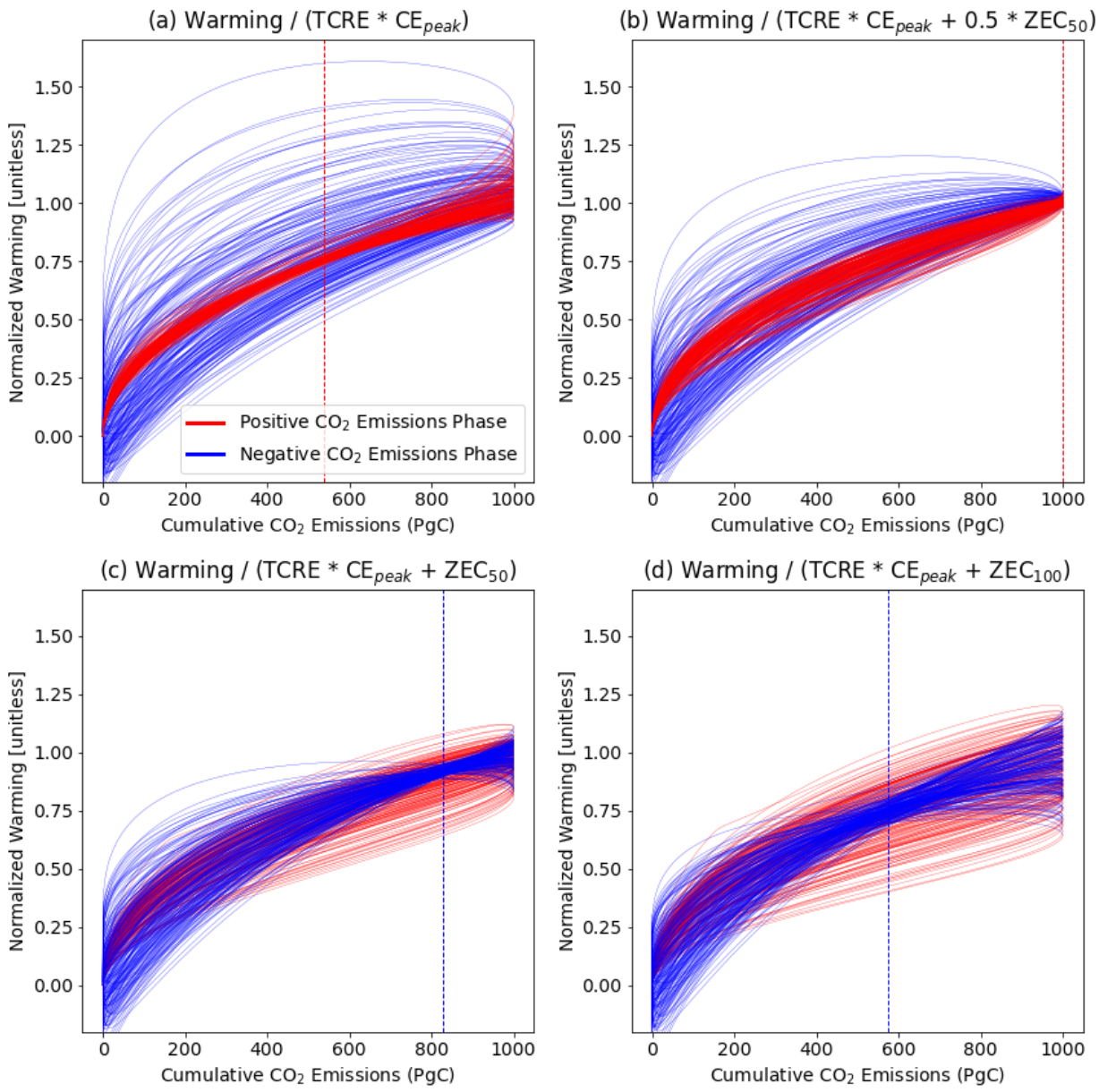

Fig. 4. Temperature vs cumulative CO_2 emissions relationship for the FaIR simple climate model ensemble driven by the idealized emissions reversal scenario. Red curves are for the positive emissions phase (years 0-150) and blue for the negative emissions phase (years 151-300) of the scenario. Panels differ in the normalization of warming for each ensemble member on the y axis, in order to show where along the trajectory each normalization minimizes the spread across the ensemble: (a) warming divided by TCRE * peak cumulative emissions (CE_{peak}, which equals 1000 PgC for all ensembles); (b) warming divided by TCRE * CE_{peak} + half of the ZEC_{50}; (c) warming divided by TCRE *CE_{peak} + ZEC_{50}; (c) warming divided by TCRE *CE_{peak} + ZEC_{100}. Positive emissions phase curves are foregrounded in panels a-b, negative emissions phase curves are foregrounded in panels c-d. Vertical dashed lines show the cumulative emissions that correspond to minimum ensemble spread in normalized temperature

across the ensemble for each panel, also colored by the emissions phase during which that minimum spread occurs (red=positive, blue=negative).

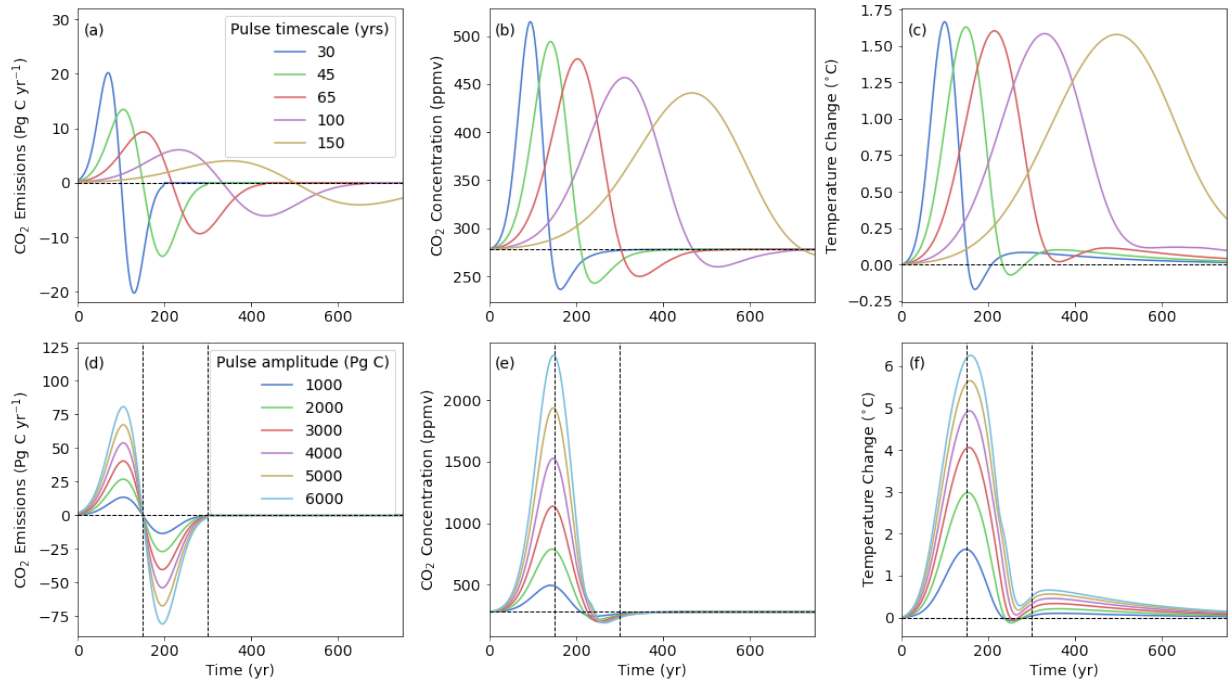

Fig. 5 Sensitivity to timescale and amplitude of forcing (a-c) sensitivity to timescale of carbon reversal in FaIR simple climate model. Reference case (all prior results) uses a 45 year pulse timescale and 1000 PgC maximum cumulative emissions. Vertical dashed lines in (d-f) note times of peak cumulative emissions and return to zero cumulative emissions.

Data availability

All CESM2 data for the experiment described here will be made available at time of publication. All scripts to generate and analyze climate model output here are available at https://github.com/ckoven/idealized_emissionsdriven_cdr_scenario.

Acknowledgements

CDK acknowledges support by the Director, Office of Science, Office of Biological and Environmental Research of the US Department of Energy under contract DE-AC02-05CH11231 through the Regional and Global Model Analysis Program (RUBISCO SFA). BS acknowledges support by H2020 programs ESM2025 (grant agreement no. 101003536) and 4C (GA 821003). ALSS acknowledges support from DOE BER RGMA award DE-SC0021209 to the University of Washington. We acknowledge the World Climate Research Programme, which, through its Working Group on Coupled Modelling, coordinated and promoted CMIP6. We thank the climate modeling groups for producing and making available their model output, the Earth System Grid Federation (ESGF) for archiving the data and providing access, and the multiple funding

agencies who support CMIP6 and ESGF. Computing resources (https://doi.org/10.5065/D6RX99HX) were provided by the Climate Simulation Laboratory at NCAR's Computational and Information Systems Laboratory, sponsored by the National Science Foundation and other agencies. We thank two anonymous reviewers for their thoughtful comments and suggestions, which improved the manuscript.

References

Allen M R, Frame D J, Huntingford C, Jones C D, Lowe J A, Meinshausen M and Meinshausen N 2009 Warming caused by cumulative carbon emissions towards the trillionth tonne *Nature* **458** 1163–6 Online: https://www.nature.com/articles/nature08019

Anderson K and Peters G 2016 The trouble with negative emissions *Science* **354** 182–3 Online: http://dx.doi.org/10.1126/science.aah4567

Archer D, Eby M, Brovkin V, Ridgwell A, Cao L, Mikolajewicz U, Caldeira K, Matsumoto K, Munhoven G, Montenegro A and Tokos K 2009 Atmospheric Lifetime of Fossil Fuel Carbon Dioxide *Annu. Rev. Earth Planet. Sci.* **37** 117–34 Online: https://doi.org/10.1146/annurev.earth.031208.100206

Arora V K, Katavouta A, Williams R G, Jones C D, Brovkin V, Friedlingstein P, Schwinger J, Bopp L, Boucher O, Cadule P, Chamberlain M A, Christian J R, Delire C, Fisher R A, Hajima T, Ilyina T, Joetzjer E, Kawamiya M, Koven C D, Krasting J P, Law R M, Lawrence D M, Lenton A, Lindsay K, Pongratz J, Raddatz T, Séférian R, Tachiiri K, Tjiputra J F, Wiltshire A, Wu T and Ziehn T 2020 Carbon–concentration and carbon–climate feedbacks in CMIP6 models and their comparison to CMIP5 models *Biogeosciences* **17** 4173–222 Online: https://bg.copernicus.org/articles/17/4173/2020/

Boucher O, Halloran P R, Burke E J, Doutriaux-Boucher M, Jones C D, Lowe J, Ringer M A, Robertson E and Wu P 2012 Reversibility in an Earth System model in response to CO2 concentration changes *Environ. Res. Lett.* **7** 024013 Online: https://iopscience.iop.org/article/10.1088/1748-9326/7/2/024013/meta

Caldeira K and Myhrvold N P 2013 Projections of the pace of warming following an abrupt increase in atmospheric carbon dioxide concentration *Environ. Res. Lett.* **8** 034039 Online: https://iopscience.iop.org/article/10.1088/1748-9326/8/3/034039/meta

CESM developers 2019 CMIP6 CESM2 esm-piControl experiment with CAM6, interactive land (CLM5), coupled ocean (POP2) with biogeochemistry (MARBL), interactive sea ice (CICE5.1), non-evolving land ice (CISM2.1), and CO2 concentration calculated Online: https://esgf-node.llnl.gov/search/cmip6/?institution_id=NCAR&source_id=CESM2&experiment_id=esm-piControl&variant_label=r1i1p1f1

Danabasoglu G, Lamarque J -F, Bacmeister J, Bailey D A, DuVivier A K, Edwards J, Emmons L K, Fasullo J, Garcia R, Gettelman A, Hannay C, Holland M M, Large W G, Lauritzen P H, Lawrence D M, Lenaerts J T M, Lindsay K, Lipscomb W H, Mills M J, Neale R, Oleson K W, Otto-Bliesner B, Phillips A S, Sacks W, Tilmes S, Kampenhout L, Vertenstein M, Bertini A, Dennis J, Deser C, Fischer C, Fox-Kemper B, Kay J E, Kinnison D, Kushner P J, Larson V E, Long M C, Mickelson S, Moore J K, Nienhouse E, Polvani L, Rasch P J and Strand W G 2020 The Community Earth System Model Version 2 (CESM2) *J. Adv. Model. Earth Syst.* **12** 106 Online: https://onlinelibrary.wiley.com/doi/abs/10.1029/2019MS001916

Eby M, Zickfeld K, Montenegro A, Archer D, Meissner K J and Weaver A J 2009 Lifetime of Anthropogenic Climate Change: Millennial Time Scales of Potential CO2 and Surface Temperature Perturbations *J. Clim.* **22** 2501–11 Online: http://dx.doi.org/DOI 10.1175/2008JCLI2554.1

Fuss S, Lamb W F, Callaghan M W, Hilaire J, Creutzig F, Amann T, Beringer T, de Oliveira Garcia W, Hartmann J, Khanna T, Luderer G, Nemet G F, Rogelj J, Smith P, Vicente J L V, Wilcox J, del Mar Zamora Dominguez M and Minx J C 2018 Negative emissions—Part 2: Costs, potentials and side effects *Environ. Res. Lett.* **13** 063002 Online: https://iopscience.iop.org/article/10.1088/1748-9326/aabf9f

Goodwin P, Williams R G and Ridgwell A 2015 Sensitivity of climate to cumulative carbon emissions due to compensation of ocean heat and carbon uptake *Nat. Geosci.* **8** 29–34 Online: http://www.nature.com/articles/ngeo2304

Hanssen S V, Steinmann Z J N, Daioglou V, Čengić M, Van Vuuren D P and Huijbregts M A J 2022 Global implications of crop-based bioenergy with carbon capture and storage for terrestrial vertebrate biodiversity *Glob. Change Biol. Bioenergy* **14** 307–21 Online: https://onlinelibrary.wiley.com/doi/10.1111/gcbb.12911

IPCC 2013 *Climate Change 2013 - The Physical Science Basis: Summary for Policymakers* Online: https://books.google.com/books/about/Climate_Change_2013_The_Physical_Science.html?hl=&id=KwFXAQAACAAJ

IPCC 2021 *Summary for Policymakers. In: Climate Change 2021: The Physical Science Basis. Contribution of Working Group I to the Sixth Assessment Report of the Intergovernmental Panel on Climate Change* ed V Masson-Delmotte, P Zhai, A Pirani, S L Connors, C Péan, S Berger, N Caud, Y Chen, L Goldfarb, M I Gomis, M Huang, K Leitzell, E Lonnoy, J B R Matthews, T K Maycock, T Waterfield, O Yelekçi, R Yu and B Zhou

John J G, Stock C A and Dunne J P 2015 A more productive, but different, ocean after mitigation *Geophys. Res. Lett.* **42** 9836–45 Online: http://doi.wiley.com/10.1002/2015GL066160

Jones C D, Ciais P, Davis S J, Friedlingstein P, Gasser T, Peters G P, Rogelj J, van Vuuren D P, Canadell J G, Cowie A, Jackson R B, Jonas M, Kriegler E, Littleton E, Lowe J A, Milne J, Shrestha G, Smith P, Torvanger A and Wiltshire A 2016 Simulating the Earth system response to negative emissions *Environ. Res. Lett.* **11** 095012 Online: https://iopscience.iop.org/article/10.1088/1748-9326/11/9/095012

Jones C D, Frölicher T L, Koven C, MacDougall A H, Damon Matthews H, Zickfeld K, Rogelj J, Tokarska K B, Gillett N P, Ilyina T, Meinshausen M, Mengis N, Séférian R, Eby M and Burger F A 2019 The Zero Emissions Commitment Model Intercomparison Project (ZECMIP) contribution to C4MIP: quantifying committed climate changes following zero carbon emissions *Geoscientific Model Development* **12** 4375–85 Online: http://dx.doi.org/10.5194/gmd-12-4375-2019

Joos F, Roth R, Fuglestvedt J S, Peters G P, Enting I G, von Bloh W, Brovkin V, Burke E J, Eby M, Edwards N R, Friedrich T, Frölicher T L, Halloran P R, Holden P B, Jones C, Kleinen T, Mackenzie F T, Matsumoto K, Meinshausen M, Plattner G-K, Reisinger A, Segschneider J, Shaffer G, Steinacher M, Strassmann K, Tanaka K, Timmermann A and Weaver A J 2013 Carbon dioxide and climate impulse response functions for the computation of greenhouse gas metrics: a multi-model analysis *Atmos. Chem. Phys.* **13** 2793–825 Online: https://acp.copernicus.org/articles/13/2793/2013/

Keller D P, Lenton A, Scott V, Vaughan N E, Bauer N, Ji D, Jones C D, Kravitz B, Muri H and

Zickfeld K 2018 The Carbon Dioxide Removal Model Intercomparison Project (CDRMIP): rationale and experimental protocol for CMIP6 *Geosci. Model Dev.* **11** 1133–60 Online: https://gmd.copernicus.org/articles/11/1133/2018/

Koven C D, Arora V K, Cadule P, Fisher R A, Jones C D, Lawrence D M, Lewis J, Lindsay K, Mathesius S, Meinshausen M, Mills M, Nicholls Z, Sanderson B M, Séférian R, Swart N C, Wieder W R and Zickfeld K 2022 Multi-century dynamics of the climate and carbon cycle under both high and net negative emissions scenarios *Earth System Dynamics* **13** 885–909 Online: https://esd.copernicus.org/articles/13/885/2022/esd-13-885-2022.pdf

Lee J Y, Marotzke J, Bala G, Cao L, Corti S, Dunne J P, Engelbrecht F, Fischer E, Fyfe J C, Jones C, Maycock A, Mutemi J, Ndiaye O, Panickal S and Zhou T 2021 Future Global Climate: Scenario-Based Projections and Near-Term Information Supplementary Material *Climate Change 2021: The Physical Science Basis. Contribution of Working Group I to the Sixth Assessment Report of the Intergovernmental Panel on Climate Change* ed V Masson-Delmotte, P Zhai, A Pirani, S L Connors, C Péan, S Berger, N Caud, Y Chen, L Goldfarb, M I Gomis, M Huang, K Leitzell, E Lonnoy, J B R Matthews, T K Maycock, T Waterfield, O Yelekçi, R Yu and B Zhou Online: https://www.ipcc.ch/

Liddicoat S K, Wiltshire A J, Jones C D, Arora V K, Brovkin V, Cadule P, Hajima T, Lawrence D M, Pongratz J, Schwinger J and Others 2020 Compatible Fossil Fuel CO2 emissions in the CMIP6 Earth System Models' Historical and Shared Socioeconomic Pathway experiments of the 21st Century *J. Clim.* 1–72 Online: https://journals.ametsoc.org/view/journals/clim/aop/JCLI-D-19-0991.1/JCLI-D-19-0991.1.xml

MacDougall A H 2019 Limitations of the 1 % experiment as the benchmark idealized experiment for carbon cycle intercomparison in C^{4}MIP *Geosci. Model Dev.* **12** 597–611 Online: https://gmd.copernicus.org/articles/12/597/2019/

MacDougall A H 2013 Reversing climate warming by artificial atmospheric carbon-dioxide removal: Can a Holocene-like climate be restored? *Geophys. Res. Lett.* **40** 5480–5 Online: http://doi.wiley.com/10.1002/2013GL057467

MacDougall A H 2016 The Transient Response to Cumulative CO2 Emissions: a Review *Current Climate Change Reports* **2** 39–47 Online: https://doi.org/10.1007/s40641-015-0030-6

MacDougall A H and Friedlingstein P 2015 The origin and limits of the near proportionality between climate warming and cumulative CO2 emissions *J. Clim.* **28** 4217–30 Online: http://journals.ametsoc.org/doi/10.1175/JCLI-D-14-00036.1

MacDougall A H, Frölicher T L, Jones C D, Rogelj J, Matthews H D, Zickfeld K, Arora V K, Barrett N J, Brovkin V, Burger F A and Others 2020 Is there warming in the pipeline? A multi-model analysis of the Zero Emissions Commitment from CO 2 *Biogeosciences* **17** 2987–3016 Online: https://bg.copernicus.org/preprints/bg-2019-492/

Matthews H D and Caldeira K 2008 Stabilizing climate requires near-zero emissions *Geophys. Res. Lett.* **35** Online: http://doi.wiley.com/10.1029/2007GL032388

Matthews H D, Gillett N P, Stott P A and Zickfeld K 2009 The proportionality of global warming to cumulative carbon emissions *Nature* **459** 829–32 Online:

https://www.nature.com/articles/nature08047

Millar R J, Nicholls Z R, Friedlingstein P and Allen M R 2017 A modified impulse-response representation of the global near-surface air temperature and atmospheric concentration response to carbon dioxide emissions *Atmos. Chem. Phys.* **17** 7213–28 Online: https://acp.copernicus.org/articles/17/7213/2017/

Proistosescu C and Huybers P J 2017 Slow climate mode reconciles historical and model-based estimates of climate sensitivity *Sci Adv* **3** e1602821 Online: http://dx.doi.org/10.1126/sciadv.1602821

Raupach M R 2013 The exponential eigenmodes of the carbon-climate system, and their implications for ratios of responses to forcings *Earth Syst. Dynam.* **4** 31–49 Online: http://www.earth-syst-dynam.net/4/31/2013/

Ricke K L and Caldeira K 2014 Maximum warming occurs about one decade after a carbon dioxide emission *Environ. Res. Lett.* **9** 124002 Online: https://iopscience.iop.org/article/10.1088/1748-9326/9/12/124002

Rogelj J, Forster P M, Kriegler E, Smith C J and Séférian R 2019 Estimating and tracking the remaining carbon budget for stringent climate targets *Nature* **571** 335–42 Online: http://dx.doi.org/10.1038/s41586-019-1368-z

Rugenstein M A A and Armour K C 2021 Three flavors of radiative feedbacks and their implications for estimating equilibrium climate sensitivity *Geophys. Res. Lett.* **48** Online: https://onlinelibrary.wiley.com/doi/10.1029/2021GL092983

Smith C J, Forster P M, Allen M, Leach N, Millar R J, Passerello G A and Regayre L A 2018 FAIR v1.3: a simple emissions-based impulse response and carbon cycle model *Geosci. Model Dev.* **11** 2273–97 Online: https://gmd.copernicus.org/articles/11/2273/2018/

Smith P, Davis S J, Creutzig F, Fuss S, Minx J, Gabrielle B, Kato E, Jackson R B, Cowie A, Kriegler E, van Vuuren D P, Rogelj J, Ciais P, Milne J, Canadell J G, McCollum D, Peters G, Andrew R, Krey V, Shrestha G, Friedlingstein P, Gasser T, Grübler A, Heidug W K, Jonas M, Jones C D, Kraxner F, Littleton E, Lowe J, Moreira J R, Nakicenovic N, Obersteiner M, Patwardhan A, Rogner M, Rubin E, Sharifi A, Torvanger A, Yamagata Y, Edmonds J and Yongsung C 2015 Biophysical and economic limits to negative CO2 emissions *Nat. Clim. Chang.* **6** 42–50 Online: https://www.nature.com/articles/nclimate2870

Solomon S, Plattner G-K, Knutti R and Friedlingstein P 2009 Irreversible climate change due to carbon dioxide emissions *Proc. Natl. Acad. Sci. U. S. A.* **106** 1704–9 Online: http://dx.doi.org/10.1073/pnas.0812721106

Thompson D W J, Barnes E A, Deser C, Foust W E and Phillips A S 2015 Quantifying the Role of Internal Climate Variability in Future Climate Trends *J. Clim.* **28** 6443–56 Online: https://journals.ametsoc.org/view/journals/clim/28/16/jcli-d-14-00830.1.xml

Tokarska K B, Gillett N P, Weaver A J, Arora V K and Eby M 2016 The climate response to five trillion tonnes of carbon *Nat. Clim. Chang.* **6** 851–5 Online: https://doi.org/10.1038/nclimate3036

Tokarska K B, Zickfeld K and Rogelj J 2019 Path independence of carbon budgets when

meeting a stringent global mean temperature target after an overshoot *Earths Future* **7** 1283–95 Online: https://onlinelibrary.wiley.com/doi/abs/10.1029/2019EF001312

Zickfeld K, Azevedo D, Mathesius S and Matthews H D 2021 Asymmetry in the climate–carbon cycle response to positive and negative CO2 emissions *Nat. Clim. Chang.* **11** 613–7 Online: http://www.nature.com/articles/s41558-021-01061-2

Zickfeld K and Herrington T 2015 The time lag between a carbon dioxide emission and maximum warming increases with the size of the emission *Environ. Res. Lett.* **10** 031001 Online: https://iopscience.iop.org/article/10.1088/1748-9326/10/3/031001

Zickfeld K, MacDougall A H and Damon Matthews H 2016 On the proportionality between global temperature change and cumulative CO2 emissions during periods of net negative CO2 emissions *Environ. Res. Lett.* **11** 055006 Online: https://iopscience.iop.org/article/10.1088/1748-9326/11/5/055006/meta

Ziehn T, Lenton A and Law R 2020 An assessment of land-based climate and carbon reversibility in the Australian Community Climate and Earth System Simulator *Mitigation and Adaptation Strategies for Global Change* **25** 713–31 Online: https://doi.org/10.1007/s11027-019-09905-1

Supplementary Information

To understand why the response of CO_2 concentrations in the atmosphere lead emissions in response to an emissions reversal, we can consider a general case of a sinusoidal emissions timeseries, that drives a combined land and ocean sink timeseries that is proportional to emissions but with an additional lag term. We can thus consider the airborne CO_2 change as the sum of two sinusoidal functions, for emissions and sinks respectively, and use the trigonometric identity for addition with arbitrary lags:

$$a\ sin(x\ +\ \theta_A)\ +\ b\ sin\ (x\ +\ \theta_B)\ = c\ sin\ (x\ +\ \varphi)$$

Whose solution terms c (amplitude) and φ (lag) are:

$$c^2\ = a^2\ +\ b^2\ +\ 2\ a\ b\ cos(\theta_A - \theta_B)$$

$$tan(\varphi) = \frac{a\ sin(\theta_A)\ +\ b\ sin(\theta_B)}{a\ cos(\theta_A)\ +\ b\ cos(\theta_B)}$$

In the case of the Earth system response to emissions, the sink magnitude *b* is approximately half of the emissions *a* (i.e. the airborne fraction is roughly ~0.5) and with a lag relative to emissions that is small relative to the timescale of emissions reversal. Thus if we set *a = 1, b = -0.5,* θ_A= 0, and use the small-angle approximation for θ_B, then we can calculate the amplitude c and lag φ of the resulting sum as:

$$c^2\ = 1.25\ -\ cos(-\theta_B)$$

$$c\ \approx 0.5$$

And

$$tan(\varphi) = \frac{-0.5\ \ sin(\theta_B)}{1\ -\ 0.5\ cos(\theta_B)}$$

$$tan(\varphi) \approx \frac{-0.5\ \theta_B}{1\ -\ 0.5}$$

$$\varphi\ \approx\ -\theta_B$$

Thus we should expect the change in atmospheric CO_2 to have roughly half the amplitude of emissions and lead the emissions by approximately the amount that the sink lags emissions, as is found in CESM2 here.

Supplementary Figures

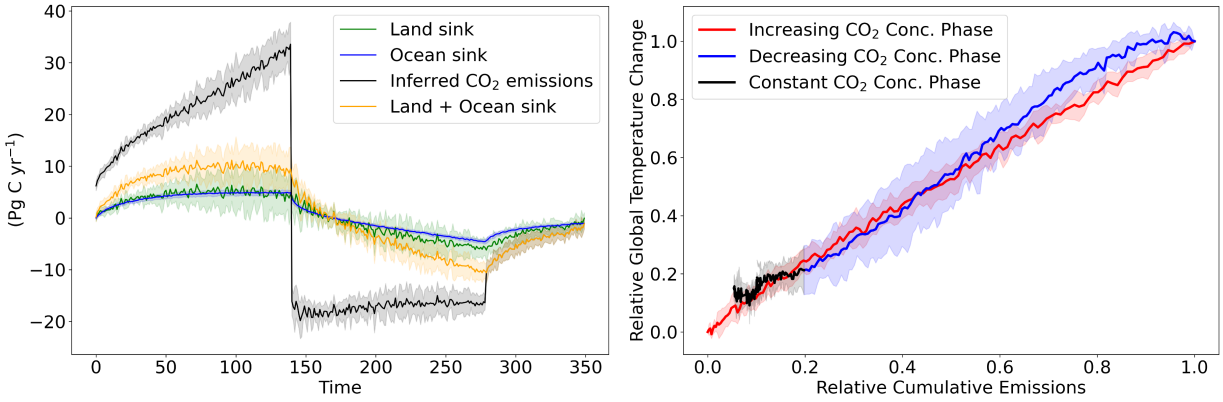

(a) (b)

Fig. S1 (a) Timeseries of land (green), ocean (blue), and combined sink (orange) fluxes, and inferred CO_2 emissions (black), for CMIP6 CDRMIP 1%/yr CO_2 concentration reversal experiment, and (b) T vs CE plot for CMIP6 1%/yr CO_2 concentration reversal CDRMIP experiment (red is for increasing CO_2 concentrations phase, blue is decreasing CO_2 concentrations phase, black is for constant CO_2 concentration phase). Solid lines are ensemble mean and shading is +/- 1σ across ensemble. 7 Earth system models used under the CDRMIP 1%/yr forcing experiment (Keller *et al* 2018): CESM2 (Danabasoglu *et al* 2020), CanESM5 (Swart *et al* 2019a), CNRM-ESM2-1(Séférian *et al* 2019), UKESM1-0-LL (Sellar *et al* 2019), ACCESS-ESM1.5 (Ziehn *et al* 2020), GFDL-ESM4 (Dunne *et al* 2020), and NorESM2-LM (Seland *et al* 2020). For all models, compatible emissions were calculated based on the sum of land carbon fluxes, ocean carbon fluxes, and atmospheric CO_2, assuming a constant conversion value of 1 ppm CO_2 = 2.124 PgC (Ballantyne *et al* 2012) for all models. Data available at: CESM2: (Danabasoglu 2019), CanESM5: (Swart *et al* 2019b), CNRM-ESM2-1: (Seferian 2021), UKESM1-0-LL: (Jones *et al* 2020), ACCESS-ESM1.5: (Ziehn *et al* 2019), GFDL-ESM4: (John *et al* 2018), and NorESM2-LM: (Tjiputra *et al* 2019).

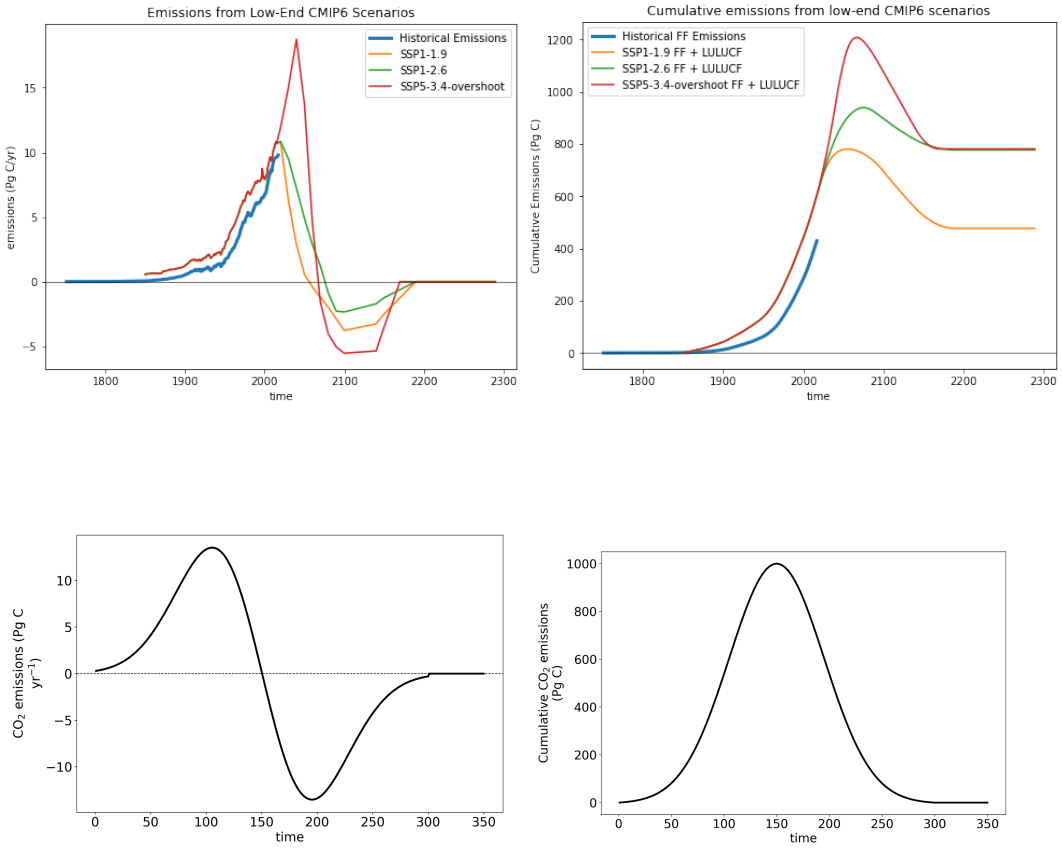

Fig. S2 (a) CO_2 emissions timeseries and (b) cumulative CO_2 emissions timeseries for SSP overshoot scenarios (c) CO_2 emissions timeseries and (d) cumulative CO_2 emissions timeseries for idealized scenario explored here.

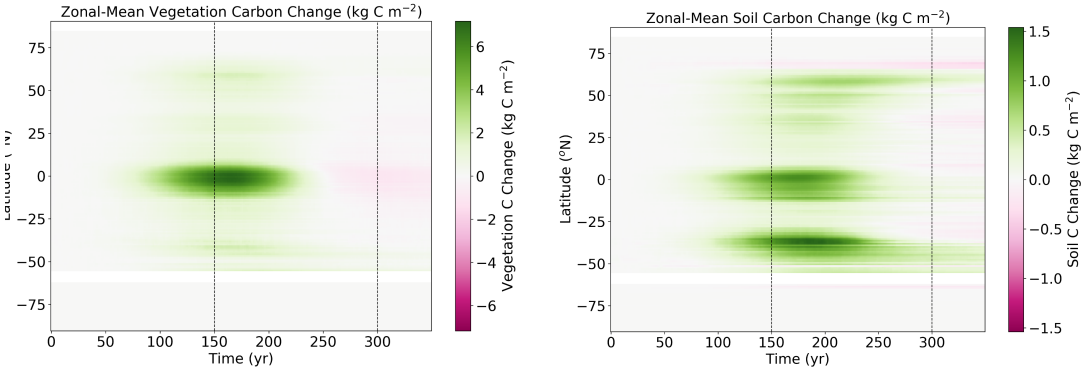

Fig. S3 Zonal-mean trajectories of (a) vegetation and (b) soil carbon change for CESM2 simulation.

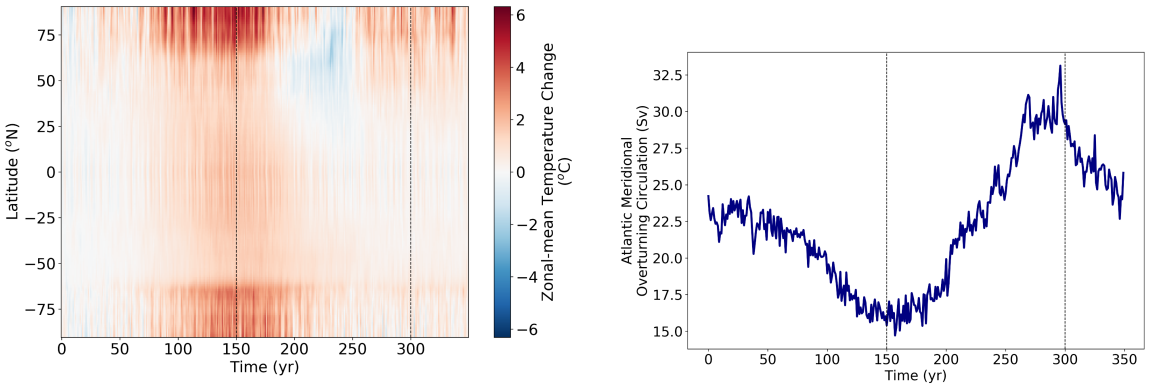

Fig. S4 (a) CESM2 Zonal-mean surface temperature anomalies, and (b) Atlantic meridional overturning circulation through the scenario.

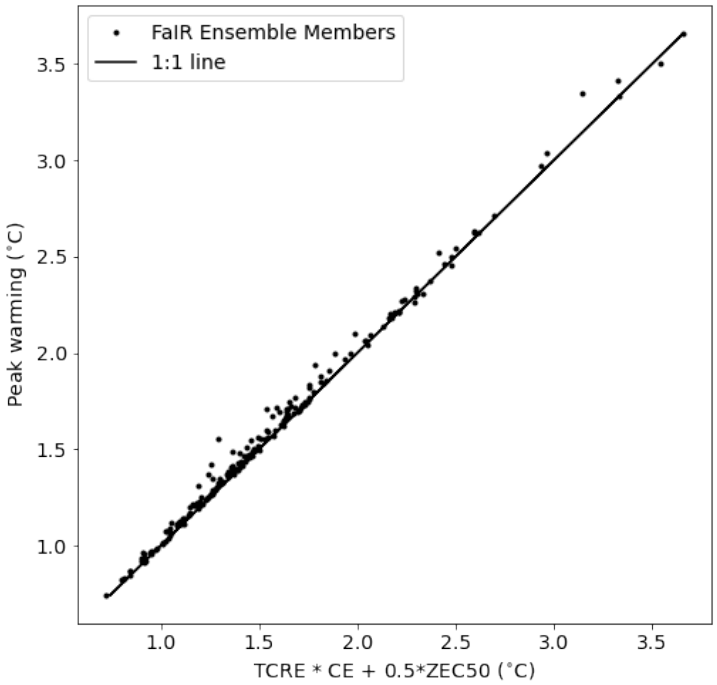

Fig S5 Scatterplot of the peak warming as predicted by TCRE * CE + 0.5* ZEC50 for each FaIR ensemble member. Also shown is the 1:1 line for comparison. Cumulative emissions (CE) are the peak value (1000 Pg C) for all ensemble members. Regression slope of the relationship is 1.003 with a an intercept of -0.01 and an r^2 of 0.994, as compared to a regression against TCRE*CE only (e.g. as in fig. 3b), which has a slope of 0.95, intercept of 0.14, and an r^2 of 0.936.

Parameter	Shape parameter	Scale parameter	5th Percentile	50th Percentile	95th Percentile
τ_0	0.6	10^6	3.6e5	1e6	2.6e6
τ_1	0.6	400	140	390	990
τ_2	0.6	100	37	100	260
τ_3	0.6	5	1.8	4.9	1.3

Table S1: Carbon sink timescale parameters (years) for lognormal distributions used in FaIR simple model ensemble.

Parameter	Shape parameter	Scale parameter	5th Percentile	50th Percentile	95th Percentile
q_0	0.6	.5	.20	.50	1.3
q_1	0.6	.33	.13	.33	.41
q_2	0.6	.41	.14	.41	1.1

Table S2: Thermal sensitivity parameters in $KW^{-1}m^2$ for lognormal distributions used in FaIR simple model ensemble.

Parameter	Shape parameter	Scale parameter	5th Percentile	50th Percentile	95th Percentile
d_0	0.6	3000	1100	3100	8200
d_1	0.6	200	70	190	520
d_2	0.6	4	1.5	4.1	10

Table S3: Thermal timescale parameters in years for lognormal distributions used in FaIR simple model ensemble.

Supplementary Material References

Ballantyne A P, Alden C B, Miller J B, Tans P P and White J W C 2012 Increase in observed net carbon dioxide uptake by land and oceans during the past 50 years *Nature* **488** 70–2 Online: http://dx.doi.org/10.1038/nature11299

Danabasoglu G 2019 NCAR CESM2 model output prepared for CMIP6 CDRMIP 1pctCO2-cdr Online: http://cera-www.dkrz.de/WDCC/meta/CMIP6/CMIP6.CDRMIP.NCAR.CESM2.1pctCO2-cdr

Danabasoglu G, Lamarque J -F, Bacmeister J, Bailey D A, DuVivier A K, Edwards J, Emmons L K, Fasullo J, Garcia R, Gettelman A, Hannay C, Holland M M, Large W G, Lauritzen P H, Lawrence D M, Lenaerts J T M, Lindsay K, Lipscomb W H, Mills M J, Neale R, Oleson K W, Otto-Bliesner B, Phillips A S, Sacks W, Tilmes S, Kampenhout L, Vertenstein M, Bertini A, Dennis J, Deser C, Fischer C, Fox-Kemper B, Kay J E, Kinnison D, Kushner P J, Larson V E, Long M C, Mickelson S, Moore J K, Nienhouse E, Polvani L, Rasch P J and Strand W G 2020 The Community Earth System Model Version 2 (CESM2) *J. Adv. Model. Earth Syst.* **12** 106 Online: https://onlinelibrary.wiley.com/doi/abs/10.1029/2019MS001916

Dunne J P, Horowitz L W, Adcroft A J, Ginoux P, Held I M, John J G, Krasting J P, Malyshev S, Naik V, Paulot F, Shevliakova E, Stock C A, Zadeh N, Balaji V, Blanton C, Dunne K A, Dupuis C, Durachta J, Dussin R, Gauthier P P G, Griffies S M, Guo H, Hallberg R W, Harrison M, He J, Hurlin W, McHugh C, Menzel R, Milly P C D, Nikonov S, Paynter D J, Ploshay J, Radhakrishnan A, Rand K, Reichl B G, Robinson T, Schwarzkopf D M, Sentman L T, Underwood S, Vahlenkamp H, Winton M, Wittenberg A T, Wyman B, Zeng Y and Zhao M 2020 The GFDL earth system model version 4.1 (GFDL-ESM 4.1): Overall coupled model description and simulation characteristics *J. Adv. Model. Earth Syst.* **12** Online: https://onlinelibrary.wiley.com/doi/10.1029/2019MS002015

John J G, Blanton C, McHugh C, Radhakrishnan A, Rand K, Vahlenkamp H, Wilson C, Zadeh N T, Dunne J P, Dussin R, Gauthier P P G, Horowitz L W, Malyshev S, Ploshay J, Stock C, Winton M and Zeng Y 2018 NOAA-GFDL GFDL-ESM4 model output prepared for CMIP6 CDRMIP 1pctCO2-cdr Online: http://cera-www.dkrz.de/WDCC/meta/CMIP6/CMIP6.CDRMIP.NOAA-GFDL.GFDL-ESM4.1pctCO2-cdr

Jones C, Liddicoat S and Wiltshire A 2020 MOHC UKESM1.0-LL model output prepared for CMIP6 CDRMIP 1pctCO2-cdr Online: http://cera-www.dkrz.de/WDCC/meta/CMIP6/CMIP6.CDRMIP.MOHC.UKESM1-0-LL.1pctCO2-cdr

Keller D P, Lenton A, Scott V, Vaughan N E, Bauer N, Ji D, Jones C D, Kravitz B, Muri H and Zickfeld K 2018 The Carbon Dioxide Removal Model Intercomparison Project (CDRMIP): rationale and experimental protocol for CMIP6 *Geosci. Model Dev.* **11** 1133–60 Online: https://gmd.copernicus.org/articles/11/1133/2018/

Seferian R 2021 CNRM-CERFACS CNRM-ESM2-1 model output prepared for CMIP6 CDRMIP 1pctCO2-cdr Online: http://cera-www.dkrz.de/WDCC/meta/CMIP6/CMIP6.CDRMIP.CNRM-CERFACS.CNRM-ESM2-1.1pctCO2-cdr

Séférian R, Nabat P, Michou M, Saint-Martin D, Voldoire A, Colin J, Decharme B, Delire C, Berthet S, Chevallier M, Sénési S, Franchisteguy L, Vial J, Mallet M, Joetzjer E, Geoffroy O, Guérémy J-F, Moine M-P, Msadek R, Ribes A, Rocher M, Roehrig R, Salas-y-Mélia D, Sanchez E, Terray L, Valcke S, Waldman R, Aumont O, Bopp L, Deshayes J, Éthé C and Madec G 2019 Evaluation of CNRM earth system model, CNRM-ESM2-1: Role of earth system processes in present-day and future climate *J. Adv. Model. Earth Syst.* **11** 4182–227 Online: https://onlinelibrary.wiley.com/doi/abs/10.1029/2019MS001791

Seland Ø, Bentsen M, Olivié D, Toniazzo T, Gjermundsen A, Graff L S, Debernard J B, Gupta A K, He Y-C, Kirkevåg A, Schwinger J, Tjiputra J, Aas K S, Bethke I, Fan Y, Griesfeller J, Grini A, Guo C, Ilicak M, Karset I H H, Landgren O, Liakka J, Moseid K O, Nummelin A, Spensberger C, Tang H, Zhang Z, Heinze C, Iversen T and Schulz M 2020 Overview of the Norwegian Earth System Model (NorESM2) and key climate response of CMIP6 DECK, historical, and scenario simulations *Geosci. Model Dev.* **13** 6165–200 Online: https://gmd.copernicus.org/articles/13/6165/2020/

Sellar A A, Jones C G, Mulcahy J P, Tang Y, Yool A, Wiltshire A, O'Connor F M, Stringer M, Hill R, Palmieri J, Woodward S, Mora L, Kuhlbrodt T, Rumbold S T, Kelley D I, Ellis R, Johnson C E, Walton J, Abraham N L, Andrews M B, Andrews T, Archibald A T, Berthou S, Burke E, Blockley E, Carslaw K, Dalvi M, Edwards J, Folberth G A, Gedney N, Griffiths P T, Harper A B, Hendry M A, Hewitt A J, Johnson B, Jones A, Jones C D, Keeble J, Liddicoat S, Morgenstern O, Parker R J, Predoi V, Robertson E, Siahaan A, Smith R S, Swaminathan R, Woodhouse M T, Zeng G and Zerroukat M 2019 UKESM1: Description and Evaluation of the U.K. Earth System Model *J. Adv. Model. Earth Syst.* **11** 4513–58 Online: https://onlinelibrary.wiley.com/doi/abs/10.1029/2019MS001739

Swart N C, Cole J N S, Kharin V V, Lazare M, Scinocca J F, Gillett N P, Anstey J, Arora V, Christian J R, Hanna S, Jiao Y, Lee W G, Majaess F, Saenko O A, Seiler C, Seinen C, Shao A, Sigmond M, Solheim L, von Salzen K, Yang D and Winter B 2019a The Canadian Earth System Model version 5 (CanESM5.0.3) *Geoscientific Model Development* **12** 4823–73 Online: https://gmd.copernicus.org/articles/12/4823/2019/gmd-12-4823-2019.pdf

Swart N C, Cole J N S, Kharin V V, Lazare M, Scinocca J F, Gillett N P, Anstey J, Arora V, Christian J R, Jiao Y, Lee W G, Majaess F, Saenko O A, Seiler C, Seinen C, Shao A, Solheim L, von Salzen K, Yang D, Winter B and Sigmond M 2019b CCCma CanESM5 model output prepared for CMIP6 CDRMIP 1pctCO2-cdr Online: http://cera-www.dkrz.de/WDCC/meta/CMIP6/CMIP6.CDRMIP.CCCma.CanESM5.1pctCO2-cdr

Tjiputra J, Schwinger J, Seland Ø, Bentsen M, Oliviè D J L, Toniazzo T, Gjermundsen A, Graff L S, Debernard J B, Gupta A K, He Y, Kirkevåg A, Aas K S, Bethke I, Fan Y, Gao S, Griesfeller J, Grini A, Guo C, Ilicak M, Karset I H H, Liakka J, Moseid K O, Nummelin A, Tang H, Zhang Z, Heinze C, Iversen T and Schulz M 2019 NCC NorESM2-LM model output prepared for CMIP6 CDRMIP 1pctCO2-cdr Online: http://cera-www.dkrz.de/WDCC/meta/CMIP6/CMIP6.CDRMIP.NCC.NorESM2-LM.1pctCO2-cdr

Ziehn T, Chamberlain M A, Law R M, Lenton A, Bodman R W, Dix M, Stevens L, Wang Y-P and Srbinovsky J 2020 The Australian Earth System Model: ACCESS-ESM1.5 *J. South. Hemisph. Earth Syst. Sci.* **70** 193 Online: http://www.publish.csiro.au/?paper=ES19035

Ziehn T, Chamberlain M, Lenton A, Law R, Bodman R, Dix M, Mackallah C, Druken K and Ridzwan S M 2019 CSIRO ACCESS-ESM1.5 model output prepared for CMIP6 CDRMIP 1pctCO2-cdr Online: http://cera-

www.dkrz.de/WDCC/meta/CMIP6/CMIP6.CDRMIP.CSIRO.ACCESS-ESM1-5.1pctCO2-cdr